Optimal Control of Virtual Batteries using Stochastic Linearization

Sarnaduti Brahma[1], Mads R. Almassalkhi[1], and Hamid R. Ossareh[1]

***Abstract*— Stochastic Linearization (SL) is a method of linearizing a nonlinearity that, unlike traditional Jacobian linearization that is valid only close to the operating point, uses statistical properties of the input to render the linearization fairly accurate over a wide range of inputs. In this paper, the method of SL is applied to optimally design controllers for an aggregation of distributed energy resources (DERs), called a virtual battery (VB), by taking into account the solar penetration levels, grid parameters, and the VB power limits. Analysis and simulation results show that VB performance can be greatly improved over a baseline design that ignores VB power limits, and that the controllers can be adaptively designed to effectively respond to changes in system parameters. This proves to be a new method for designing controllers to improve the participation of power-constrained VBs.**

I. INTRODUCTION

With increased penetration of renewable generation like solar photovoltaic (PV), coordinated control of demand-side distributed energy resources (DERs) in distribution feeders is becoming vital to supporting a clean energy future. Many works in this area propose novel control architectures to coordinate and control these resources. For example, in [1], [2], methods for load frequency control using DERs are described. In [3], the active and reactive power of DERs are controlled using information exchange with neighboring DERs, while in [4], a model predictive control-based approach is taken. Moreover, a virtual battery (VB) is an abstraction, i.e., a modeling tool, to capture the flexibility and dynamics of aggregations of DERs [5]–[7] that enables analysis and design of controllers. Generally, the objective of VB control (ignoring grid constraints) is to maximize revenue [8]. Hence, if the output power of the VBs are controlled, as we seek to achieve this objective, the VBs may be pushed to their energy or power limits. This requires controller design to be cognizant of power/energy limits.

While most works on hierarchical control of DERs (e.g. [9]) mainly consider using frequency and voltage droop characteristics to generate power set-points for DERs using local measurements of frequency and voltage and compensating for the deviations, in [10], a previous work by the authors, a novel hierarchical framework for control of VBs in distribution feeders was proposed, wherein the deviation in the *head node* power of the feeder from an *economic* trajectory was minimized instead. Unlike most local droop-based control strategies that are generally not cognizant of the network, the design of the controller gains was done based on the grid topology and device constraints, using the concept of a VB, with power and energy saturation limits, to represent an aggregation of DERs.

Existing works to tune controller parameters based on saturation limits are either heuristic [10], or the parameters are not optimized [11], which means the full potential of VBs is not unleashed. Furthermore, no work adaptively retunes the controller parameters to take into account variable saturation levels using real-time data. In the case of tuning PID controllers [12], there exist methods like the Cohen Coon, Internal Model Control, and Ziegler Nichols, but they also do not provide a mechanism to include the saturation nonlinearity in the design process. From a technical standpoint, the challenge is that saturation represents a nonlinearity and the grid is driven by stochastic inputs, a class of systems for which control design tools are limited.

While there exist methods for analysis and design of nonlinear systems in their original form [13], they are usually hard to implement in practice. Hence, the usual practice is to perform Jacobian linearization of the system at an operating point, by evaluating the gradient of the nonlinear function at the operating point and replacing the nonlinearity with an affine approximation at that point, and then leverage the methods of linear systems theory [14], [15]. However, such an approximation is valid only *locally* and fails to approximate the behavior in the case of stochastic inputs that may drive the system away from the operating point. Quasilinear Control (QLC) is a recently developed theory for the analysis and design of nonlinear systems driven by stochastic inputs [16], [17]. It is based on Stochastic Linearization (SL), which is a method of linearizing a nonlinearity using the statistical properties of the input to the nonlinearity. Unlike traditional Jacobian linearization, on which linear control is based, SL is a *global* method of linearization that takes into account both the parameters of the nonlinear system and the statistical properties of the exogenous signals driving the system.

There is a significant body of literature in the field of SL. An overview of the prominent works can be found in [18], [19]. The theory of QLC applies SL to nonlinear feedback systems frequently encountered by control engineers, extending traditional control techniques like the root-locus design to stochastic systems [16], [17], [20], [21]. In [16], the nonlinearities considered are single-variable and symmetric, while in [17], [20], QLC was extended to asymmetric nonlinearities. QLC was extended to multivariate nonlinearities in [22]. SL has been applied to various control systems with saturation in [20] and time-delays in [21]. In [23], a previous work by the authors, SL was applied for optimal primary frequency control of power systems with a single generator saturation.

In this paper, the technique of SL is leveraged to optimally control VBs. Specifically, this paper illustrates the advantages of using an SL-based optimization compared to the optimal VB controller described in [10], [24]. While existing design methods (for linear controller design of systems with saturation) based on Lyapunov functions and LMIs [13], [25] treat the saturation as a sector-

[1]The authors are with the Department of Electrical and Biomedical Engineering, The University of Vermont, VT 05405, USA. Email Addresses: {sbrahma, malmassa, hossareh}@uvm.edu

bounded nonlinearity and, hence, lead to conservative designs, our goal is to achieve a non-conservative, optimal design, though with a small approximation error due to SL. Specifically, we show in this paper that compared to a baseline design, SL results in more accurate estimation of signal statistics, SL-based optimization can reduce head node power deviation from nominal while optimizing VB usage, and that SL-based optimization can use updated information to update the controller parameters, i.e., can be made adaptive. Thus, the original contributions of this paper are:

- An SL-based optimal controller design for control of networked VBs with fixed power limits (i.e., by modeling the limits by a univariate saturation function),
- Adaptive SL-based design of VB controllers using real-time data,
- Analysis on the effect of various system parameters on the optimization, and
- Simulation-based analysis of the SL-based design to VBs with variable power limits (i.e., by modeling the limits by a trivariate saturation function).

The outline of the rest of the paper is as follows. Section II describes the modeling of VBs and the optimization problem. Section III briefly reviews SL. Section IV showcases the advantages of an SL-based optimization over a non-SL based optimization in improving VB usage while attaining the grid objective. In Section V, analyses are provided to explore the effect of various parameters on the capabilities of this method. Section VI extends the design to VBs with variable power limits. Finally, Section VII concludes the paper.

II. Modeling and Problem Formulation

A. Virtual Battery Model

In this paper, aggregated DERs are modeled as a VB (consistent with abstractions in [5], [26], [27]) with a saturation in power delivered, defined by the lower and upper power limits, $P_{\min}$ and $P_{\max}$, respectively. The VB is assumed to be operating at a nominal power set-point denoted by P_{set} (which can be computed, for example, optimally at a slower time-scale, as described in [10]). The input and output of the VB are related by the following transfer function:

$$\frac{P_u(s)}{P_{\text{in}}(s)} = \frac{e^{-T_d s}}{\tau s + 1} \tag{1}$$

where $P_u(s)$ is the Laplace transform of the unsaturated output of the VB, $p_u(t)$, and $P_{\text{in}}(s)$ that of the power desired (input) from the VB, $p_{\text{in}}(t)$, τ is a first-order lag, and T_d is a pure time delay.

The model of (1) is obtained by taking into account the following facts [10]: i) The DERs composing a VB turn on/off (possibly) sequentially, and power electronic components present inside each VB, both contribute to a net lag τ; ii) There are communication delays (generally of the order of 200 ms) between the head node of the feeder and each VB [28], [29], and delays associated with disaggregating the control signal into device-level signals [30]. The delays we consider in the VB model (T_d) are of both these types lumped together.

Defining $u(t) := P_u(t) - P_{\text{set}}$, the saturated output of the VB is then $P_b(t) = P_{\text{set}} + \text{sat}_\alpha^\beta(u(t))$, where $\alpha := P_{\min} - P_{\text{set}}$,

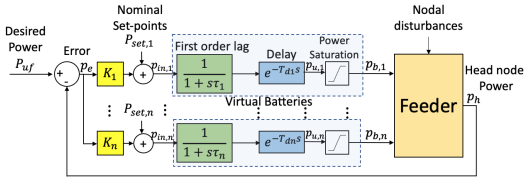

Fig. 1: Nonlinear Feedback System

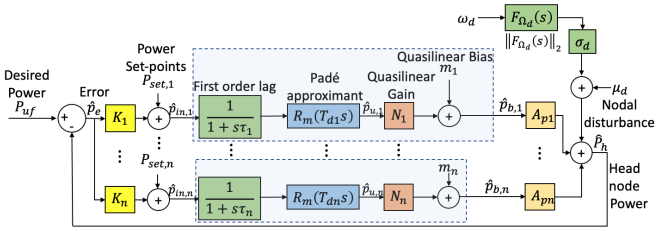

Fig. 2: Stochastically Linearized System

$\beta := P_{\max} - P_{\text{set}}$, since the DC gains of the first-order transfer function and of the time delay are both unity, and

$$\text{sat}_\alpha^\beta(u) = \begin{cases} \beta, & u \geq \beta \\ u, & \alpha < u < \beta \\ \alpha, & u \leq \alpha \end{cases}. \tag{2}$$

B. Problem Setup

Consider a distribution feeder with sets of distributed energy resources (DERs) modeled by VBs (as in the previous subsection) located at its various nodes. The objective is to control the head node active power demand of the feeder, such that it tracks an economic reference by rejecting uncontrolled nodal disturbances, using available flexibility of the DERs. The control scheme is shown in Fig. 1, and is adapted from [10]. It consists essentially of a bank of proportional controllers K_i that multiply the error between the head node power $p_h(t)$ of the feeder and a desired economic trajectory $P_{uf}(t)$ to control the ith VB with the model described in Section II-A (with suffix i added in all the parameters).

As described in [10], [24], the gains K_i in Fig. 1 can be designed optimally by first (Jacobian) linearizing the feeder at an operating point, depending on the nominal set-point $P_{\text{set},i}$ of the ith VB and the base load, neglecting the power saturation in the VBs (see Fig. 2, but with $N_i = 1$ and $m_i = 0$ - these will be defined later - essentially, this means locally linearizing all saturations and removing them from the analysis). This linearization leads to gains A_{pi}, which indicate the sensitivities of the head node active power of the feeder to the corresponding nodal active power injections. Next, a stationary Gaussian stochastic process is assumed as nodal disturbance (representing aggregate random fluctuations in solar PV over possibly a large geographic region [31]) with mean μ_d and standard deviation (SD) σ_d, and an mth order Padé approximation $R_m(T_{di}s)$ is assumed for the delay. The gains are then chosen by minimizing the sum of the variance of the tracking error, $\hat{p}_e(t)$, denoted by $\sigma^2_{\hat{p}_e}$, and a weighted sum of the variances of the control inputs to the VBs, $\hat{p}_{\text{in},i}(t)$, denoted by $\sigma^2_{\hat{p}_{\text{in},i}}$:

$$\text{minimize} \, \sigma^2_{\hat{p}_e} + \rho \sum_{i=1}^{n} \sigma^2_{\hat{p}_{\text{in},i}} \tag{3}$$

where the variances are computed using the $\mathcal{H}_2$-norm of the transfer functions from the standard white Gaussian noise $w_d(t)$

to $\hat{p}_e(t)$ and $\hat{p}_{\text{in},i}(t)$ (setting $\mu_d = 0$), and $\rho > 0$ is a constant chosen according to the power capacity of the VBs.

However, the optimization problem (3) does not include the saturation nonlinearities due to VB power limits. Note that while the nonlinear feeder can be linearized with Jacobian linearization, the saturation nonlinearities in the VBs cannot. This is because the power flows in the nonlinear system due to nodal injections are close to that predicted by the linearized feeder and do not change their region of operation drastically. However, when VBs are nearly saturated, even a small disturbance can change the region of operation (by saturating), rendering a Jacobian linearization inaccurate. Moreover, although the control penalty ρ can be chosen to be inversely proportional to the power capacity of the VBs, as done in [10], it is difficult to choose it according to the saturation level of the VBs and is rather heuristic. Hence, the focus of this paper is to overcome these problems by leveraging SL instead of Jacobian linearization to linearize the saturation functions. The method of SL provides a method to *systematically* include the saturation authorities and the saturation level (based on the operating point) of the VBs into the optimization problem. Also, it utilizes the statistical properties of the disturbance signal to linearize the system. In the next section, the procedure of SL is reviewed before using it to solve the above problem.

III. Brief Review of Stochastic Linearization

A. Open-Loop

Consider a nonlinear system described by the following input-output relationship $v(t) = f(u(t))$, where $u(t)$ is a stationary Gaussian random process, $v(t)$ is the output and $f : \mathbb{R} \to \mathbb{R}$ is a piece-wise differentiable function satisfying the following properties [32]:

1) $\frac{\partial f}{\partial u}$ exists and is continuous almost everywhere;
2) $|f(u)| < A\exp(u^a)$, $a < 2$, for some $A \in \mathbb{R}$ and any $u \in \mathbb{R}$.

The above properties essentially ensure that the derivative of $f(\cdot)$ is integrable, which is required for the derivation of the SL coefficients. Please refer to [32] for details.

The objective of SL is to approximate this nonlinearity by $\hat{v}(t) = Nu_0(t) + M$, where $u_0(t) = u(t) - \mu_u$ is the zero-mean part of the input $u(t)$, μ_u the mean of $u(t)$ and $\hat{v}(t)$ the output of the linear approximation, such that the mean square difference $E[(v - \hat{v})^2]$ is minimized [17], [19]. Here the parameter N is called the *quasilinear gain* and M the *quasilinear bias*. For convenient block diagram manipulation, it is convenient to evaluate $m = M - N\mu_u$, such that $\hat{v}(t) = Nu(t) + m$ (since, in a control system, we do not have ready access to $u_0(t)$, but to $u(t)$). It can be shown [17]:

$$N = E[f'(u(t))], \quad M = E[f(u(t))] \tag{4}$$

where the expectation is taken with respect to the probability density function (PDF) of the input $u(t)$.

Specifically, for the saturation nonlinearity defined in (2), which is piece-wise differentiable, the values of N and M can be computed from:

$$N = \frac{1}{2}\left[\text{erf}\left(\frac{\beta - \mu_u}{\sqrt{2}\sigma_u}\right) - \text{erf}\left(\frac{\alpha - \mu_u}{\sqrt{2}\sigma_u}\right)\right] =: \mathcal{F}_N(\mu_u, \sigma_u) \tag{5}$$

$$M = \frac{\alpha + \beta}{2} + \frac{\mu_u - \beta}{2}\text{erf}\left(\frac{\beta - \mu_u}{\sqrt{2}\sigma_u}\right) - \frac{\mu_u - \alpha}{2}\text{erf}\left(\frac{\alpha - \mu_u}{\sqrt{2}\sigma_u}\right) - \frac{\sigma_u}{\sqrt{2\pi}}\left\{\exp\left[-\left(\frac{\beta - \mu_u}{\sqrt{2}\sigma_u}\right)^2\right] - \exp\left[-\left(\frac{\alpha - \mu_u}{\sqrt{2}\sigma_u}\right)^2\right]\right\} =: \mathcal{F}_M(\mu_u, \sigma_u) \tag{6}$$

where σ_u is the SD of $u(t)$, $\text{erf}(x) = \frac{2}{\sqrt{\pi}}\int_0^x e^{-t^2} dt$ is the error function, and $\mathcal{F}_N(\cdot,\cdot)$ and $\mathcal{F}_M(\cdot,\cdot)$ are functions defined to show the dependence of N and M on μ_u and σ_u. For more details, please refer to [17], [20].

B. Closed-Loop

Now consider that the nonlinearity $f(\cdot)$ is present inside a closed-loop system that is otherwise linear. As can be seen from (4), to find the SL of this nonlinearity, we need the PDF of the input to this nonlinearity, $u(t)$. However, since the input signal depends on the nonlinearity's output through the feedback loop, such PDF is not readily available. Hence, we assume that the system has been stochastically linearized and that the moments (specifically, the mean μ_u and SD, σ_u) of the input to the nonlinearity, $u(t)$, are approximated by the corresponding moments of the corresponding input $\hat{u}(t)$ ($\mu_{\hat{u}}$ and $\sigma_{\hat{u}}$) in the linearized system (this leads to only a small error for plants with a low-pass filtering nature [17]), and proceed with the SL of the nonlinearity as in the open-loop case using (4) [18]. However, note that, in this case, $\mu_{\hat{u}}$ and $\sigma_{\hat{u}}$ themselves depend on N and M due to feedback and can be written as a function of system parameters and reference/disturbance statistics using the $\mathcal{H}_2$-norm and DC gains of the corresponding transfer functions, as shown in the next section. Hence, closed-loop SL involves solving the following transcendental equations in N and M:

$$N = \mathcal{F}_N(\mu_{\hat{u}}(M), \sigma_{\hat{u}}(N)), \quad M = \mathcal{F}_M(\mu_{\hat{u}}(M), \sigma_{\hat{u}}(N)) \tag{7}$$

where $\mathcal{F}_N$ and $\mathcal{F}_M$ are as defined in (5)-(6). MATLAB®'s `fsolve` command provides a convenient way to solve these equations numerically. This completes the process of SL.

IV. Optimal Controller Design for Virtual Batteries using Stochastic Linearization

In this section, the procedure of SL is applied to the optimal controller design for VBs, and simulation results are shown to illustrate the effectiveness of the approach.

A. Formulation using SL

Leveraging the method of SL, the nonlinear system in Fig. 1 can be approximated using (7) by an equivalent linear system shown in Fig. 2, where the saturation function for the ith VB, $\text{sat}_{\alpha_i}^{\beta_i}(u_i)$, has been replaced by an equivalent quasilinear gain N_i and a bias $m_i = M_i - N_i\mu_{\hat{u}_i}$ such that M_i is the quasilinear bias and $\mu_{\hat{u}i}$ is the mean of the input to the saturation, $\hat{u}_i(t) = P_{\hat{u},i}(t) - P_{\text{set},i}$.

As seen from (7), calculation of N_i, M_i requires knowledge of $\mu_{\hat{u}i}$, and $\sigma_{\hat{u}i}$, and hence, these variables depend on each other and all other system parameters. Considering that the system is operating in the stationary regime, the values of $\sigma_{\hat{u}i}$ can be found using the transfer function from the nodal disturbance $w_d(t)$ to $\hat{P}_{u,i}(t)$:

$$\sigma_{\hat{u}i} = \left\| \frac{F_{\Omega_d}(s) K_i \frac{1}{1+s\tau_i} R_m(T_{di}s)}{1 + \sum_{i=1}^{n} K_i \frac{1}{1+s\tau_i} R_m(T_{di}s) N_i A_{pi}} \right\|_2 \sigma_d \tag{8}$$

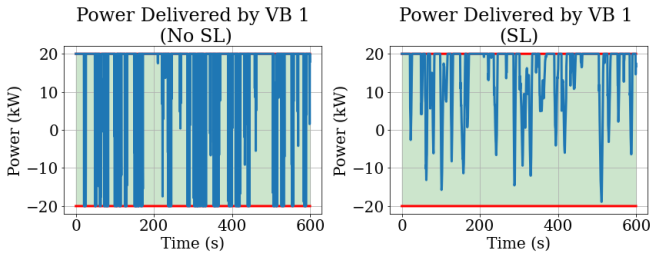

(a) VB Usage - No SL

(b) VB Usage - SL

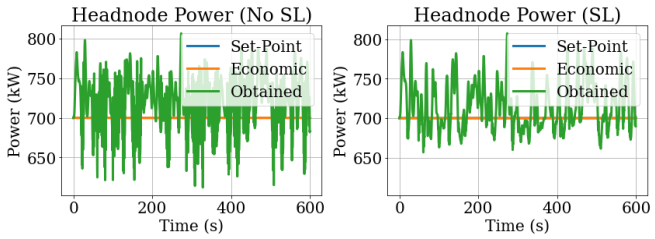

(c) Head node power - No SL

(d) Head node power - SL

Fig. 3: VB Usage and Head Node Power. This is for VBs with fixed power limits (i.e., univariate saturation).

The values of $\mu_{\hat{u}_i}$ can be obtained by finding the transfer functions from μ_d, and m_i to $\hat{P}_{u,i}(t)$ and evaluating their DC gains, which leads to:

$$\mu_{\hat{u}i} = (P_{uf} - \mu_d - \sum_{j=1}^{n} M_j A_{pj}) K_i \tag{9}$$

where M_j are functions of $\mu_{\hat{u}i}$ and $\sigma_{\hat{u}i}$, obtained using (6).

The values of N_i, M_i can thus be found by substituting (8)-(9) into (7) for each N_i, M_i, $\sigma_{\hat{u}i}$ and $\mu_{\hat{u}_i}$, which results in a system of $2n$ transcendental equations in the unknowns N_i and M_i, for $i = 1,...,n$. Note that compared to Jacobian linearization, which assumes $N_i = 1$, $m_i = 0$, SL provides $0 < N_i < 1$ and m_i not necessarily 0, such that the statistical properties of the signals in the linearized system and the nonlinear system match closely. Thus, SL-based optimization involves formulating the optimization problem described in (3) by *considering* the values of N_i, M_i (and thus $m_i = M_i - N_i \mu_{\hat{u}i}$) while evaluating $\sigma_{\hat{P}_e}$ and $\sigma_{\hat{P}_{\text{in},i}}$:

$$\begin{aligned} &\text{minimize} && \sigma^2_{\hat{P}_e} + \rho \textstyle\sum_{i=1}^{n} \sigma^2_{\hat{P}_{\text{in},i}} \\ &\text{subject to:} && (8),(9), i = 1,2,...,n \\ & && N_i = \mathcal{F}_N(\mu_{\hat{u}}(M_i), \sigma_{\hat{u}i}(N_i)), i = 1,2,...,n \\ & && M_i = \mathcal{F}_M(\mu_{\hat{u}}(M_i), \sigma_{\hat{u}i}(N_i)), i = 1,2,...,n \end{aligned} \tag{10}$$

where:

$$\sigma_{\hat{P}_e} = \left\| \frac{F_{\Omega_d}(s) K_i}{1 + \sum_{i=1}^{n} K_i \frac{1}{1+s\tau_i} R_m(T_{di}s) N_i A_{pi}} \right\|_2 \sigma_d$$

and $\sigma_{\hat{P}_{\text{in},i}} = K_i \sigma_{\hat{P}_e}$.

Note that (10) defines a static optimization problem that is dependent on system parameters (like σ_d) that can be estimated and/or measured. If the system parameters change, the optimization can be re-done. This adaptive nature of SL is discussed in more detail in Section IV-C.

B. Simulation

1) Setup: The simulation setup consists of an IEEE 37-node feeder (single-phase equivalent) [33], with two VBs at two different nodes (specifically, 701 and 737), where the base loads are 140 kW each. The upper and lower power limits of the VBs are taken to be 20 kW and -20 kW respectively. The nominal power set-points are optimally found to be 20 and 18 kW (using the optimal set-point dispatcher described in [10]) to meet a head node power demand of 700 kW, resulting in a highly saturated system. The maximum state-of-charge capacities of the VBs were taken to be 80 kWh (representing a maximum of four hours of operation at maximum power capacity) each. The time constants of the first-order VB model were taken to be 600 ms and 400 ms respectively, and the time delays to be 100 ms and 200 ms respectively. We assume Gaussian random active and reactive power noise injected into certain locations of the feeder (as is expected, for example, due to random cloud cover). A 10 min simulation was performed using both the SL-based optimization and the non-SL-based optimization to illustrate the effectiveness of SL. The value of ρ was assumed to be 0.1 and a 3rd order Padé approximation was considered for the delays in both cases.

TABLE I: Signal Statistics

Quantity	With No SL	With SL	Improvement (%)
SD of VB 1 Power (P)	15.2 kW	9.9 kW	35.2
SD of VB 2 P	14.8 kW	10.3 kW	30.1
Mean of Head Node P	713.8 kW	709.2 kW	0.6
SD of Head Node P	33.9 kW	30.0 kW	11.8
Cost	3609.3 kW^2	1121.9 kW^2	68.9

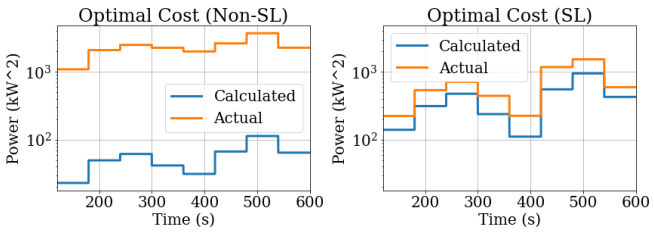

(a) Non-SL

(b) SL

Fig. 4: Optimal Cost, evaluated over one minute intervals. Y-axis is in log scale.

2) Results and Discussion: Fig. 3 shows the power delivered by one of the VBs, both by not using SL (Fig. 3a) and using SL (Fig. 3b). It can be seen that there is significant saturation using the controller gains designed without SL. This is because there is no knowledge of VB power bounds in that design. Moreover, the variability of the head node power shown in Fig. 3c is also high. However, with SL-based design, the saturation and variability of VB power are significantly reduced, along with a reduction in the head node power deviation (Fig. 3d) from the desired value of 700 kW. The mean and SDs of the signals were found numerically after the simulations, and the improvements are summarized in Table I. Note that although a single simulation is reported here to illustrate the effectiveness of SL, other simulations performed with the similar conditions also resulted in similar improvements with SL. Of course, the exact system parameters will dictate how effective SL will be in a given situation, and we discuss the effect of some system parameters in Section V.

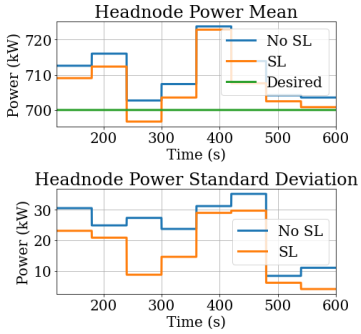

Fig. 5: Headnode power. Statistics are evaluated over one minute intervals.

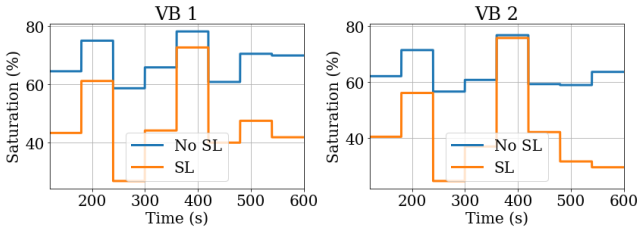

(a) Non-SL (b) SL

Fig. 6: Saturation of VBs

C. Data Driven SL Formulation

Since the SL process mentioned in the previous section takes into account all system parameters (as in (10)), the controller gains can be designed *adaptively*, considering changes in system parameters (such as saturation limits in VB power) or exogenous signal statistics (such as the mean and SD of the head node power). In situations when these parameters can be estimated using real-time data, e.g., using Kalman filters, recursive least squares, or running averages [34]), the controller gains can be adaptively re-tuned based on this data. If done sufficiently slowly, the system stability is not comprised, though the proof of this is a topic for future research. This subsection illustrates the effectiveness of SL for adaptive control of VBs by using updated head node power statistics at regular intervals.

1) Setup: The same system is considered as described in Section IV-B.1. However, in this case, the disturbance statistics μ_d and σ_d are estimated over a running window of two minutes using measured head node statistics and the linearized system model. The VB optimization problem is run every minute using updated head node power (over the last two minutes), first by not using SL and then using SL. As before, ρ was assumed to be 0.1 in both cases.

2) Results and Discussion: First, the results indicate several advantages of an SL-based optimization over a non-SL based optimization. For instance, Fig. 4 shows the calculated (using (8)-(10)) and actual optimal cost (by numerical simulation) over every one minute interval. It can be seen that non-SL based optimization method *grossly underestimates* the cost that it minimizes (Fig. 4), by more than an order of magnitude, whereas the SL based optimization, due to knowledge of updated VB bounds and noise statistics, estimates the cost more accurately. Moreover, using the improved estimation of the statistics of the error and the control input in SL-based optimization, a slightly lower value of SD can be obtained and the mean of the head node power with SL is also slightly

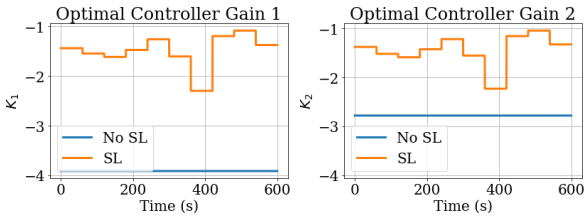

(a) Controller Gain 1 (b) Controller Gain 2

Fig. 7: Controller Gains

closer to the desired value (Fig. 5). The mean is lower due to the additional bias term that is added due to SL in the operating points of the VBs. With SL, the amount of saturation in VB power is reduced by about 10-30% (Fig. 6), indicating that VBs are being pushed lesser to their limits. This is a major advantage of an SL-based design compared to the non-SL-based design and results in much lesser usage of power to achieve the same or better grid objective.

Second, the adaptive nature of SL is specifically highlighted in Fig. 7. Unlike the non-SL based optimization, whose solution (i.e., optimal gains) is independent of noise statistics or VB bounds (since σ_d^2 is just a multiplying factor for, and μ_d does not feature in, the objective function (10), while $N_i = 1$ and $m_i = 0$ always), the SL-based optimization takes into account this information about the system to find the quasilinear gain/bias and updates the gain accordingly (Fig. 7). Hence, the SL-based optimization is adaptive, unlike the non-SL based optimization.

V. Analysis on Effect of Parameters

In this section, we provide the results of simulations to show the effect of various system parameters on the SL-based optimization procedure. This provides various insights into the design and analysis of nonlinear stochastic systems using SL.

A. Effect of Control Penalty

First, the value of the control penalty ρ is varied. In this specific study, the delay is neglected. This is because delays are not accurately modeled when the bandwidth of the control system is high, which can occur with high values of controller gains, or due to modeling errors resulting from discrete-time simulation of the continuous-time system, unless the sampling time is very small.

The effect of ρ on the optimal cost is displayed in Fig. 8a. The solid lines show the value of the cost obtained numerically from a 10-minute simulation of the VBs, while the dotted lines show the calculated cost. It can be seen that with small ρ, the non-SL-based design is not able to reduce the actual cost due to no knowledge of bounds. Effectively, for very small ρ, the control input is not penalized much, and hence its variability is high and the VB ouput is saturated. For large ρ, the costs from both the non-SL and the SL-based optimizations converge since, for large ρ, the control action is highly penalized, and thus there is no VB saturation. However, SL captures the cost more accurately due to the knowledge of bounds, and hence, it can make the actual cost smaller even for small values of ρ.

B. Effect of the number of VBs

Since SL involves solving a system of transcendental equations, the computational complexity increases as the number of

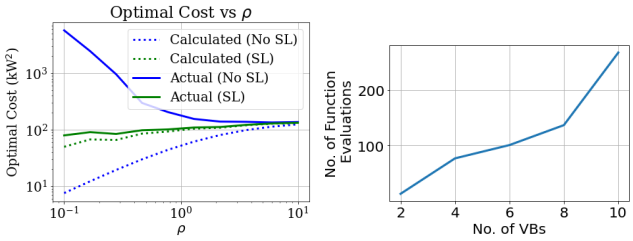

(a) Effect of ρ. Axes are in log scale. (b) No. of SL function evaluations vs. number of VBs

Fig. 8: Effect of VBs on SL and optimization

equations increases. For each VB added, there are added two equations involving N_i and M_i. To quantify the computational complexity, the number of evaluations of the SL functions for fixed controller gains were noted as the number of VBs were increased. This would roughly indicate a lower bound on the number of evaluations required of the SL functions when they are part of the optimization problem as equality constraints, as solving the optimization problem involves finding a solution to these SL equations. The equations were solved using a modification of the Powell hybrid method, as implemented in MINPACK [35] (other numerical methods were also tried, like the Broyden method, but this was the best in terms of the number of function evaluations). The results are shown in Fig. 8b. It can be seen that with the increase in the number of VBs, the number of function evaluations (for solving SL equations with fixed controller gains) also increases, indicating that SL becomes more computationally expensive, but grows polynomially rather than exponentially.

VI. Extension to Variable Virtual Battery Power Bounds

A. Modeling

In practice, the power limits of the VB's underlying DER aggregation are generally not constant [7]. The DERs that make up a VB can choose not to participate in providing grid services due to user preferences or to avoid Quality-of-Service (QoS) violations, leading to a change in the power and energy limits. To deal with such a case, a *trivariate* saturation in the VB model can be considered, where instead of the saturation authorities α and β being constants in (2), they are time-varying, i.e., $\alpha(t)$ and $\beta(t)$:

$$\text{sat}_{\alpha(t)}^{\beta(t)}(u(t)) = \begin{cases} \beta(t), & u(t) \geq \beta(t) \\ u(t), & \alpha(t) < u < \beta(t) \\ \alpha(t), & u(t) \leq \alpha(t) \end{cases} \tag{11}$$

when $\alpha(t) < \beta(t)$, and 0 otherwise (since then there is no flexibility and the VB output is nominal, i.e., $p_b(t) = P_{\text{set}}$).

B. Multivariable SL

1) Open-Loop: Equation (11) describes a trivariate nonlinearity. To find SL of this nonlinearity, (4) is not applicable. Hence, we apply the procedure of multivariable SL described in [22], where instead of (4), the quasilinear gain N *vector* and the bias M are computed for a *multivariate* function $f\colon \mathbb{R}^n \to \mathbb{R}$ using:

$$N = E[\nabla f(u(t))] := \mathcal{G}_N(\mu, \Sigma), \quad M = E[f(u(t))] := \mathcal{G}_M(\mu, \Sigma) \tag{12}$$

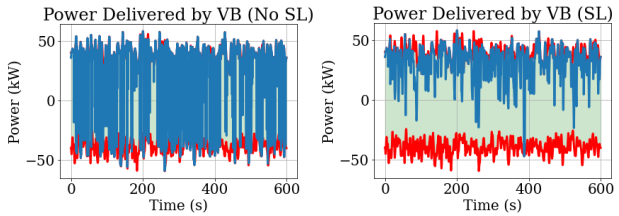

(a) No SL (b) With SL

Fig. 9: VB Actuation. The red lines indicate time-varying power limits.

where $\mathcal{G}_N(\cdot,\cdot)$ and $\mathcal{G}_M(\cdot,\cdot)$ are functions representing the dependence of N and M on μ and Σ, the mean and covariance matrix of $u(t)$ respectively. Note that μ is composed of μ_u, μ_α, and μ_β (the means of the inputs $u(t)$, $\alpha(t)$, and $\beta(t)$, respectively), and the covariance matrix Σ is composed of σ_u, σ_α, and σ_β (their corresponding SDs), and $\rho_{u\alpha}$, $\rho_{\alpha\beta}$, and $\rho_{u\beta}$ (the correlation coefficient between $u(t)$ and $\alpha(t)$, that between $\alpha(t)$ and $\beta(t)$, and that between $u(t)$ and $\beta(t)$ respectively). Assuming that $\alpha(t)$, $\beta(t)$, and $u(t)$ form a trivariate Gaussian process, on substituting the nonlinear function (11) for $f(\cdot)$ in (12), the value of N can be found as follows: $N = [N_1\ N_2\ N_3]^{\mathrm{T}} = E[\nabla \text{sat}(u(t),\alpha(t),\beta(t))]$. Here note that since the saturation function is not differentiable at certain points, the gradient ∇ has to be taken piecewise.

2) Closed-Loop: Now consider the feedback system of Fig. 1, but with trivariate saturation in VBs instead of univariate saturation. Since $\alpha_i(t)$ and $\beta_i(t)$ are intrinsic properties of the ith VB and are not influenced by the nodal disturbance $d(t)$, we assume that the values of $\mu_{\alpha i}$, $\mu_{\beta i}$, $\sigma_{\alpha i}$, $\sigma_{\beta i}$, $\rho_{u\alpha i}$, $\rho_{\alpha\beta i}$, and $\rho_{u\beta i}$ are known (based on, e.g., historical data), and evaluate $\mu_{\hat{u}i}$ and $\sigma_{\hat{u}i}$ as before from (8)-(9), in place of μ_{ui} and σ_{ui} (due to the same reason mentioned in Section III-B). Then, similar to (7), the SL of the closed-loop system is performed by solving:

$$N_i = \mathcal{G}_N(\hat{\mu}_i(M), \hat{\Sigma}_i(N)), \quad M_i = \mathcal{G}_M(\hat{\mu}_i(M), \hat{\Sigma}_i(N))$$

where $\hat{\mu}_i$ and $\hat{\Sigma}_i$ in the stochastically linearized system denote the moments corresponding to μ_i and Σ_i in the nonlinear system. This completes the SL procedure of the closed-loop system. For more details, please refer to [22].

C. Simulation

1) Setup: To illustrate the SL of the system with trivariate saturation, an IEEE 37-node feeder with a VB of 600 ms time constant and 100 ms time delay at one of its nodes was considered for the simulation. The time-varying upper and lower power limits of the VB were taken to Gaussian, with 40 and -40 kW as mean respectively, and 6 kW as the SD (for both limits). For the optimization, the value of ρ was taken to be 0.1. The power limits were assumed to be uncorrelated to the input to the saturation.

2) Results: The results are shown in Fig. 9. It can be seen that with SL, the VB power is significantly less variable than that by not using SL. The SD of the VB power in case of no SL is 28.5 kW and that with SL is 14.9 kW (an improvement of 47.7%). The mean head node power with no SL is 715.1 kW and with SL is 710.2 kW (an improvement of 0.7%) while the SD of the head node power with no SL is 32.6 kW and with SL, it is 29.7 kW (an improvement of 8.9%). The overall cost function improved

from 9826.5 kW^2 (no SL) to 1042.3 kW^2 (SL), an improvement of 89%. Moreover, it was observed that if the VB power limits were *not* assumed stochastic while designing the controller gains, but in reality they were, the actual optimal cost would increase by 2.3%, the SD of VB power by 6%, and the head node power mean by 0.1%. These serve as preliminary results to illustrate that variable power bounds can be handled in the context of VBs. A full exposition of this idea is a topic for the future.

VII. Conclusion

In this paper, an SL-based method of optimizing the power delivered by VBs in distribution feeders is described. Since SL takes into account VB power limits and other system parameters, it provides a superior method of analysis and design of gains optimally. Simulation results show that compared to a non-SL-based optimization, SL results in a more accurate estimation of signal statistics. They also indicate that SL-based optimization can reduce head node power deviation from the nominal while optimizing VB usage and can use updated information to change the gains, i.e., is adaptive. Some analysis on the effect of the control penalty ρ in the cost function shows that even at small values of this parameter, with proper models of the devices, SL can lead to a reduction in the cost. Moreover, it is shown that with an increased number of VBs, the computational complexity of SL increases. Finally, the design is extended to VBs with variable power limits. Future work includes conducting studies on the numerical efficiency of the process, and design using a discrete-time version of SL.

ACKNOWLEDGMENT

The authors would like to thank Dr. Nawaf Nazir at The University of Vermont for the implementation of the optimal economic set-point dispatch of VBs.

References

[1] A. Ghafouri, J. Milimonfared, and G. B. Gharehpetian, "Coordinated control of distributed energy resources and conventional power plants for frequency control of power systems," *IEEE Transactions on Smart Grid*, vol. 6, no. 1, pp. 104–114, 2015.

[2] V. R. Pandi, A. Al-Hinai, and A. Feliachi, "Coordinated control of distributed energy resources to support load frequency control," *Energy conversion and management*, vol. 105, pp. 918–928, 2015.

[3] A. D. Dominguez-Garcia, C. N. Hadjicostis, and N. H. Vaidya, "Resilient networked control of distributed energy resources," *IEEE Journal on Selected Areas in Communications*, vol. 30, no. 6, pp. 1137–1148, 2012.

[4] E. Mayhorn, K. Kalsi, M. Elizondo, W. Zhang, S. Lu, N. Samaan, and K. Butler-Purry, "Optimal control of distributed energy resources using model predictive control," in *2012 IEEE Power and Energy Society General Meeting*, 2012, pp. 1–8.

[5] J. T. Hughes, A. D. Domínguez-García, and K. Poolla, "Identification of virtual battery models for flexible loads," *IEEE Transactions on Power Systems*, vol. 31, no. 6, pp. 4660–4669, 2016.

[6] F. Ju, J. Wang, J. Li, G. Xiao, and S. Biller, "Virtual battery: A battery simulation framework for electric vehicles," *IEEE Transactions on Automation Science and Engineering*, vol. 10, no. 1, pp. 5–15, 1 2013.

[7] S. P. Nandanoori, I. Chakraborty, T. Ramachandran, and S. Kundu, "Identification and validation of virtual battery model for heterogeneous devices," in *2019 IEEE Power Energy Society General Meeting (PESGM)*, 2019, pp. 1–5.

[8] K. Dietrich, J. M. Latorre, L. Olmos, and A. Ramos, "Modelling and assessing the impacts of self supply and market-revenue driven virtual power plants," *Electric Power Systems Research*, vol. 119, pp. 462–470, 2015.

[9] A. Bidram and A. Davoudi, "Hierarchical structure of microgrids control system," *IEEE Transactions on Smart Grid*, vol. 3, no. 4, pp. 1963–1976, 2012.

[10] S. Brahma, N. Nazir, H. Ossareh, and M. Almassalkhi, "Optimal and resilient coordination of virtual batteries in distribution feeders," *IEEE Transactions on Power Systems*, pp. 1–1, 2020.

[11] F. Dörfler, J. Simpson-Porco, and F. Bullo, "Breaking the Hierarchy: Distributed Control & Economic Optimality in Microgrids," *IEEE Transactions on Control of Network Systems*, vol. 3, no. 3, pp. 241–253, 1 2014.

[12] K. J. Åström, T. Hägglund, and K. J. Astrom, *Advanced PID control*. ISA-The Instrumentation, Systems, and Automation Society Research Triangle Park, 2006, vol. 461.

[13] A. Isidori, *Nonlinear control systems*, 3rd ed. Springer, 1995.

[14] W. M. Wonham, "On a matrix riccati equation of stochastic control," *SIAM Journal on Control*, vol. 6, no. 4, pp. 681–697, 1968.

[15] A. J. Krener and A. Isidori, "Linearization by output injection and nonlinear observers," *Systems & Control Letters*, vol. 3, no. 1, pp. 47–52, 1983.

[16] S. Ching, Y. Eun, C. Gokcek, P. T. Kabamba, and S. M. Meerkov, *Quasilinear control: Performance analysis and design of feedback systems with nonlinear sensors and actuators*. Cambridge University Press, 2010.

[17] P. Kabamba, S. Meerkov, and H. Ossareh, "Stochastic linearisation approach to performance analysis of feedback systems with asymmetric nonlinear actuators and sensors," *International Journal of Control*, vol. 88, no. 1, pp. 65–79, 2015.

[18] L. Socha, *Linearization methods for stochastic dynamic systems*. Springer Science & Business Media, 2007, vol. 730.

[19] J. B. Roberts and P. D. Spanos, *Random Vibration and Statistical Linearization*. Dover Publications, 2003.

[20] Y. Guo, P. T. Kabamba, S. M. Meerkov, H. R. Ossareh, and C. Y. Tang, "Quasilinear Control of Wind Farm Power Output," *IEEE Transactions on Control Systems Technology*, vol. 23, no. 4, pp. 1555–1562, July 2015.

[21] W.-P. Huang, S. Brahma, and H. R. Ossareh, "Quasilinear Control of Systems with Time-Delays and Nonlinear Actuators and Sensors," in *American Control Conference (ACC)*, Philadelphia, 2019.

[22] S. Brahma and H. R. Ossareh, "Quasilinear Control of Feedback Systems with Multivariate Nonlinearities," in *58th IEEE Conference on Decision and Control (CDC)*, Nice, France, 2019.

[23] S. Brahma, M. R. Almassalkhi, and H. R. Ossareh, "A stochastic linearization approach to optimal primary control of power systems with generator saturation," in *2018 IEEE Conference on Control Technology and Applications (CCTA)*, 2018, pp. 982–987.

[24] M. Almassalkhi, S. Brahma, N. Nazir, H. Ossareh, P. Racherla, S. Kundu, S. P. Nandanoori, T. Ramachandran, A. Singhal, D. Gayme, and et al., "Hierarchical, grid-aware, and economically optimal coordination of distributed energy resources in realistic distribution systems," *Energies*, vol. 13, no. 23, p. 6399, Dec 2020.

[25] S. Boyd and H. Hindi, "Analysis of Linear Systems With Saturation Using Convex Optimization," *Proceedings of the 37th IEEE Conference on Decision and Control*, pp. 903–908, 1998.

[26] H. Hao, B. M. Sanandaji, K. Poolla, and T. L. Vincent, "Aggregate flexibility of thermostatically controlled loads," *IEEE Transactions on Power Systems*, vol. 30, no. 1, pp. 189–198, 2014.

[27] L. A. D. Espinosa, A. Khurram, and M. R. Almassalkhi, "A virtual battery model for packetized energy management," in *2020 59th IEEE Conference on Decision and Control (CDC)*, 2020, pp. 42–48.

[28] B. Naduvathuparambil, M. C. Valenti, and A. Feliachi, "Communication delays in wide area measurement systems," in *Proceedings of the Thirty-Fourth Southeastern Symposium on System Theory (Cat. No.02EX540)*, 2002, pp. 118–122.

[29] M. Amini and M. Almassalkhi, "Investigating delays in frequency-dependent load control," in *2016 IEEE Innovative Smart Grid Technologies - Asia (ISGT-Asia)*, 2016, pp. 448–453.

[30] S. P. Nandanoori, S. Kundu, D. Vrabie, K. Kalsi, and J. Lian, "Prioritized threshold allocation for distributed frequency response," in *2018 IEEE Conference on Control Technology and Applications (CCTA)*, 2018, pp. 237–244.

[31] R. Perez, M. David, T. E. Hoff, M. Jamaly, S. Kivalov, J. Kleissl, P. Lauret, and M. Perez, "Spatial and temporal variability of solar energy," *Foundations and Trends® in Renewable Energy*, vol. 1, no. 1, pp. 1–44, 2016.

[32] T. S. Atalik and S. Utku, "Stochastic linearization of multi-degree-of-freedom non-linear systems," *Earthquake Engineering & Structural Dynamics*, vol. 4, no. 4, pp. 411–420, 1976.

[33] K. P. Schneider, B. A. Mather, B. C. Pal, C. Ten, G. J. Shirek, H. Zhu, J. C. Fuller, J. L. R. Pereira, L. F. Ochoa, L. R. de Araujo, R. C. Dugan, S. Matthias, S. Paudyal, T. E. McDermott, and W. Kersting, "Analytic considerations and design basis for the ieee distribution test feeders," *IEEE Transactions on Power Systems*, vol. 33, no. 3, pp. 3181–3188, 2018.

[34] D. Simon, *Optimal state estimation: Kalman, H infinity, and nonlinear approaches*. John Wiley & Sons, 2006.

[35] J. J. Moré, B. S. Garbow, and K. E. Hillstrom, "User guide for MINPACK-1," Argonne Nat. Lab., Argonne, IL, Tech. Rep. ANL-80-74, Aug 1980.